Journal of Applied Polymer Science

Nitrile rubber/hindered phenol exterminated hyperbranched polyester materials with improved damping and mechanical performance

Yuan Yang,[1] Yun-Feng Zhao,[1,2] Mao-Sheng Zhan,[1] Jian-Yue Wang,[2] Chuan Zhao,[2] Xiao-Yan Liu,[2] Ji-Hua Zhang[2]

[1]Key Laboratory of Aerospace Materials and Performance (Ministry of Education), School of Materials Science and Engineering, Beihang University, Beijing, China

[2]Aerospace Research Institute of Materials and Processing Technology, Beijing 100076, China

Correspondence to: Y.-F. Zhao (E-mail: zhaoyf703@163.com) and M.-S. Zhan (E-mail: zhanms@buaa.edu.cn)

ABSTRACT: Hindered phenol exterminated hyperbranched polyester (mHBP) is fabricated by esterification reaction. The mHBP is introduced into nitrile rubber (NBR) to prepare NBR/mHBP blends. Structure, damping and mechanical properties of NBR/mHBP blends are investigated by Fourier transform infrared spectroscopy (FTIR), ^{1}H-NMR, dynamic mechanical thermal analyzer (DMTA), and tensile tester. FTIR spectra of the blends illustrate the intermolecular hydrogen bonding between the NBR and mHBP, contributing to the improvement of damping and mechanical properties. The results indicate that, with the increasing mHBP content, the T_g of the blends shifted to a higher temperature with a broadening temperature range and improved mechanical properties, showing an application in adjusting the T_g and temperature range without decreasing of loss factor. © 2015 Wiley Periodicals, Inc. J. Appl. Polym. Sci. **2015**, *132*, 42605.

KEYWORDS: dendrimers; elastomers; hyperbranched polymers and macrocycles; rubber; viscosity and viscoelasticity

Received 1 December 2014; accepted 7 June 2015

DOI: 10.1002/app.42605

INTRODUCTION

Viscoelastic polymers have been used as damping materials due to their outstanding properties for reducing vibration and noise around the glass transition temperature (T_g).[1] In real applications, vibrations in wide temperature and frequency range are often experienced, and a broad damping temperature range is required. However, viscoelastic polymers usually exhibit a narrow range of only 20−30°C around their T_g peak, which obstructs further application.[2] Great researches[3–5] have been made to broaden the damping temperature range of viscoelastic damping materials. Traditional modification methods to broaden the damping temperature range included copolymerization, interpenetration polymers networks, and blending of various polymers. Introducing resins, such as phenol resin,[6,7] polyvinyl chloride,[8,9] *et al.*, into rubber are the most popular methods to broaden the $\triangle T$, while the loss factor peak decreased significantly.[10] On the other hand, low molecular hindered phenols can improve the T_g peak for the strong intermolecular interactions between functional groups of hindered phenol and the matrix.[11] However, the low molecular organic fillers usually tend to decrease the toughness and stability of damping materials, which may restrict its application.[12] Xiang *et al.*[13] found that AO-80 modified NBR/PVC crosslinking composites showed an improvement of tan δ from 0.96 to 1.56 with increasing AO-80 content from 0 to 50 phr attributing to the hydrogen bonding between the AO-80 and NBR, while the elongation at break decreased from 600% to about 400% with increasing AO-80 content. Hyperbranched polymer (HBPs), a special type of dendritic polymers, have drawn great attention in recent years owing to their unique architecture, excellent flow and processing properties, and low melting and viscosity in comparison to linear polymer with the comparable molar mass. Moreover, HBPs possess abundant functional end groups, playing a major role in further reactivity, which are believed to be responsible for the enhanced toughness,[13,14] thermal resistance,[15,16] and flame retardant,[17,18] *et al.* All of these make them ideal as promising candidates for the modification of polymer materials. Recently, many articles on application of hyperbranched polymers over thermoset resin modification were published.[19–21] Helena Bergenudd *et al.*[22] prepared three different generations hyperbranched phenolic based on hyper-branched polyester Boltorn^R (H20, H30, H40) and 3-(3,5-Di-tert-butyl-4-hydroxy-phenyl)-propionic acid, the products were used as antioxidants. Similar research has been reported in literature.[23] However, as is known to me, little studies have been reported the application of hyperbranched polymers on rubber

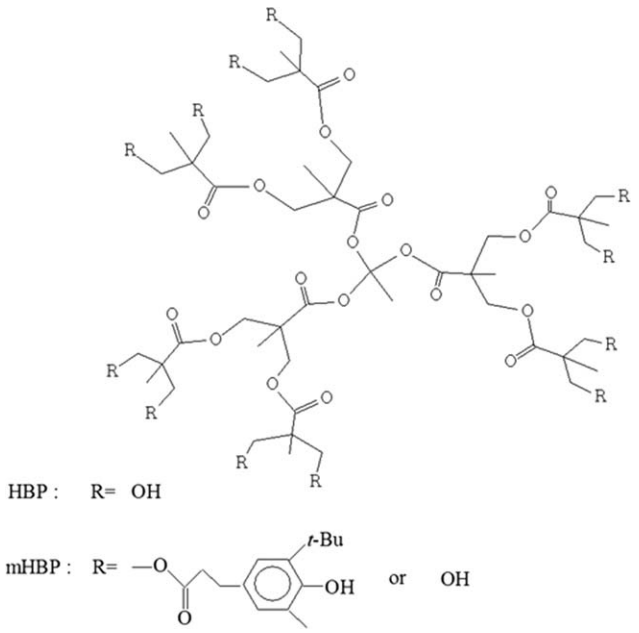

Figure 1. Structure of hyperbranched polyester.

modification,[22,23] especially about the damping properties of hyperbranched polymer-modified rubber systems.

In this article, hyperbranched polyester, modified with hindered phenol, were prepared through esterification reaction and introduced into nitrile rubbers (NBR) to prepare nitrile rubber/hyperbranched polyester hybrid materials. Structure, damping, and mechanical properties of the binary blends were studied by FTIR, ^{1}H-NMR, DMTA, and tensile tester. The blends, without decreasing T_g peak, exhibit improved damping temperature range and mechanical properties.

EXPERIMENTAL

Materials

Hyperbranched polyester (HBP), with hydroxyl group number of 12 and molecular weight of 1250 (shown in Figure 1), was purchased from Suzhou HyperT Resin Science & Technology. NBR with acrylonitrile content of 27%, was supplied by Lanzhou petrochemical company. P-toluenesulfonic acid (p-TSA), Zinc oxide (ZnO), Stearic acid (SA), Tetramethylthiuram disulfide (TMTD), 2, 2′-dibenzothiazoledisulfde (DM), Carbon black (CB), sulphur (S) were chemical pure.

Preparation of mHBP

The mHBP was prepared through a melting esterification methods, shown in Scheme 1.

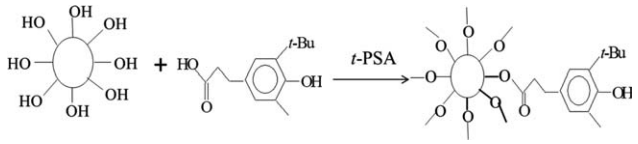

Scheme 1. Scheme of mHBP preparation.

HBP 12.5 g (0.01 mol) and 3-(3-methyl-5-tert-butyl-4-hydroxyphenyl)propionic acid (AO) 28.4 g (0.48 mol) were added into a 500 mL three-neck round-bottom flask equipped with a mechanical stirrer, reflux condenser and thermometer under nitrogen protection. The mixture was heated to 130°C. Then, p-TSA 0.4 g was added when the above mixture was melted. The reaction was maintained at 13°C for 3 h and then for another 2 h under reduced pressure to obtain the crude product. Finally, the crude product was smashed in mortar, then the powder was washed by acetone/deionized water (v/v = 1/1) mixture solution, finally dried at 80°C. The process of "smashing-washing-drying" repeated for five times to obtain the pure product.

Preparation of NBR/mHBP Blends

NBR was plasticated with a mixing roller at room temperature for 5 min, and then, calculated amount of mHPB, carbon black, ZnO, SA, TMTD, DM, S was added and the mixture was kneaded for another 10 min. The mixtures were hot-pressed and vulcanized at 150°C under the pressure of 10 MPa for 30 min to prepare the sample for measuring. Various mHBP content cured NBR blends were prepared as Table I following the above cure process.

Characterization

FTIR spectra of mHBP and NBR/mHBP blends were recorded on a Bruker Vertex 70V spectrometer at temperature from 400 to 4000 cm^{-1}.

The ^{1}H-NMR spectra was collected using a Bruker V600 spectrometer, and solvent was $CDCl_3$.

Damping properties were performed with a DMTA (Metravib R.D.S. VA4000) at 125 Hz from −50°C to 100°C in the tensile configuration.

The tensile strength, elongation at break, and percentage deformation of the samples were measured on a electronic universal testing machine (Sintech65/G, MTS), using dumb-bell shape samples according to GB/T 528-92. Hardness of the samples was performed on a LX-A Shore A durometer. The samples were tested without any conditioning.

Table I. Recipe of NBR/mHBP Blends

Sample no.	NBR (g)	HBP (g)	mHBP (g)	ZnO (g)	SA (g)	TMTD (g)	DM (g)	CB (g)	S (g)
NBR	100	0	0	5	2	1	0.5	40	2
NBR/10 HBP	100	10	0	5	2	1	0.5	40	2
NBR/10 mHBP	100	0	10	5	2	1	0.5	40	2
NBR/30 mHBP	100	0	30	5	2	1	0.5	40	2
NBR/50 mHBP	100	0	50	5	2	1	0.5	40	2

The morphology of tensile fracture was evaluated on a scanning electronic microscope (S440, Leica Cambridge) under acceleration voltage of 15 kV.

RESULTS AND DISCUSSION

FTIR and ^{1}H-NMR Spectra of mHBP

Figure 2 shows the FTIR and ^{1}H-NMR spectra of mHBP. In the spectra of mHBP, the peak (3430 cm^{-1}) attributing to —CH_2—OH of HBP shifted to 3500 cm^{-1}, attributing to Ph—OH; a new peak at 1600 cm^{-1} attributed to the C=C (aromatic) stretching; the multi peaks in the range of 1200−1250 cm^{-1} and 800−850 cm^{-1} belonged to tertiary butyl groups. In the ^{1}H-NMR spectra of mHBP, there was the peak ($\delta = 7.8$ ppm) assigning to Ph—OH; the peak ($\delta = 6.7-6.8$ ppm) belonged to the Ph-H; the peaks ($\delta = 2.0-2.3$, 2.5−2.8 ppm) corresponded to CH_2 and the peaks ($\delta = 1.1-1.4$ ppm) belonged to CH_3. From the FTIR and ^{1}H-NMR spectra of mHBP it can be seen that the hindered phenol group was grafted to the end of HBP.

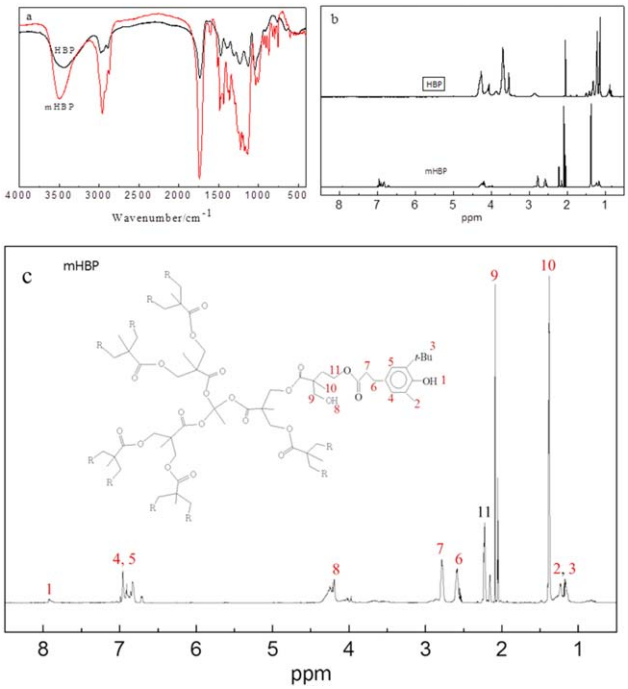

Figure 2. FTIR (a), ^{1} H-NMR spectra of HBP and mHBP (b), ^{1} H-NMR spectra and molecular structure of mHBP (c). [Color figure can be viewed in the online issue, which is available at wileyonlinelibrary.com.]

FTIR Spectra of NBR/mHBP Blends

Figure 3(a) showed the major feature of the infrared spectrum of NBR/mHBP blends with various content of mHBP. The hydroxy group (OH) stretching region near 3400 cm^{-1} and the carbonyl group (C=O) stretching region near 1730 cm^{-1} were shown in Figure 3, respectively. Corresponding to NBR/HBP blends, the hydrogen group stretching region shifted from 3330 cm^{-1} to 3450 cm^{-1} [Figure 3(a)], and the carbonyl group stretching region also shifted from 1724 cm^{-1} to 1735 cm^{-1} [Figure 3(b)]. With the increasing mHBP content, both the OH and C=O stretching region are strengthened.

As showing in Figure 3, the band at 3330 cm^{-1} was assigned to the "free" hydroxy group (nonhydrogen-bonded),[7] while the band at 3450 cm^{-1} is corresponding to "OH—C≡N" interaction, indicating that the hydrogen bonding was formed. As seen in Figure 3(b), the band of C=O group stretching vibration shifted from 1724 cm^{-1} to 1735 cm^{-1}, indicating that no intermolecular hydrogen bonding was formed between C=O and OH of mHBP with the increasing mHBP content. The formed

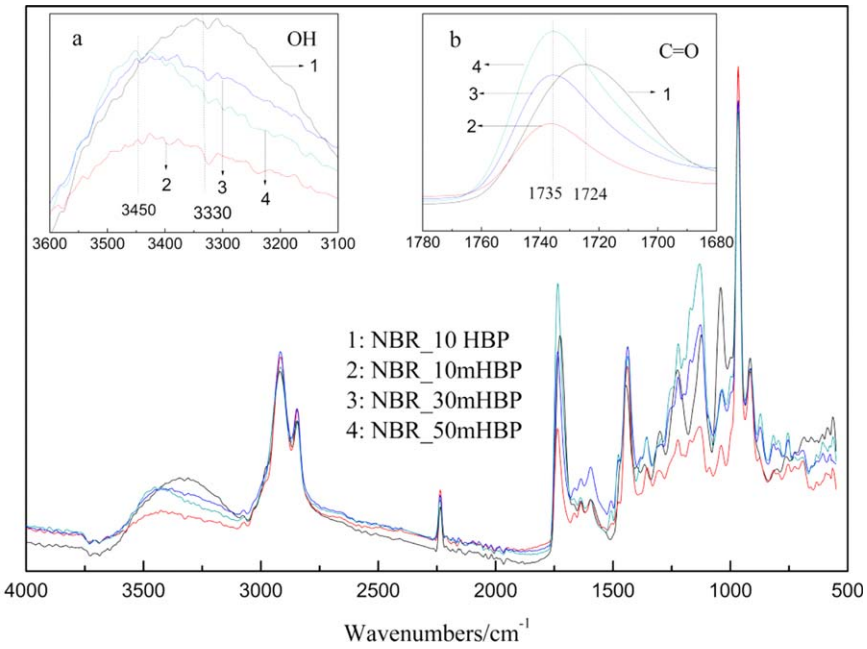

Figure 3. FTIR spectra of unvulcanized NBR/mHBP blends. [Color figure can be viewed in the online issue, which is available at wileyonlinelibrary.com.]

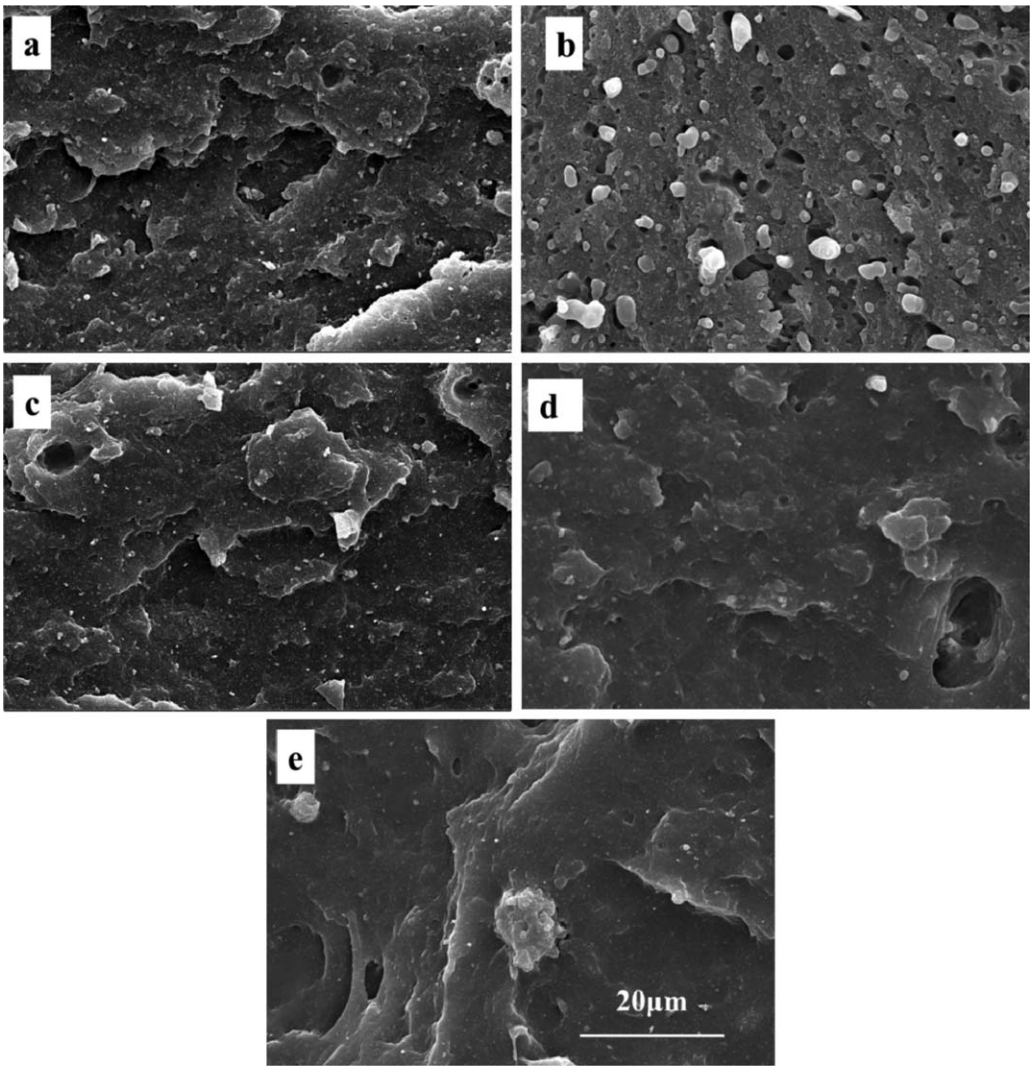

Figure 4. Morphology of tensile fracture samples. (a) NBR; (b) NBR/10HBP; (c) NBR/10mHBP; d- NBR/30mHBP; e- NBR/50mHBP

hydrogen bonds contributed to the increasing damping and mechanical properties for NBR/mHBP blends, according with literature.[24]

Morphology Analysis

The tensile fracture morphology of NBR/mHBP (or HBP) blends was investigated by SEM. The morphology pictures of all samples were illustrated in Figure 4. From Figure 4(b), it was clear that NBR/HBP sample exhibited a significant incompatibility "sea-island-structure", in which the continuous phase is NBR and HBP (white blocks) is the "island". The poor interface between NBR and HBP indicated that they were incompatible, which could explain the second loss factor peak and the decrease in tensile strength. On the contrast, as shown in Figure 4(c,d), the fracture morphology of NBR/mHBP blends became smoother without phase separation when the mHBP content increased from 0phr to 30phr, showing excellent compatibility between NBR and mHBP due to the hydrogen bonds between NBR and mHBP; however, when mHBP content further increased to 50phr, as shown in Figure 4(e), mHBP enrichment (white block) indicated the partly compatibility between NBR and mHBP.[25,26]

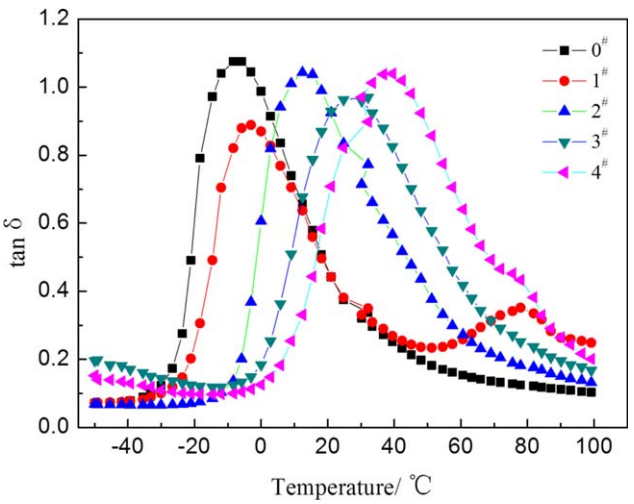

Figure 5. Temperature dependence of loss factor. $0^{\#}$ -NBR; $1^{\#}$ -NBR/10HBP; $2^{\#}$ - NBR/10mHBP; $3^{\#}$ - NBR/30mHBP; $4^{\#}$ - NBR/50mHBP. [Color figure can be viewed in the online issue, which is available at wileyonlinelibrary.com.]

Table II. Dynamic Mechanical Properties of NBR/mHBP Blends

Materials	Tan δ	T_g (°C)	$\triangle T$ (°C)	TA
NBR	1.08	−8.4	51.4	54
NBR/10 mHBP	1.04	12.4	59.4	55
NBR/30 mHBP	0.97	28.6	63	59
NBR/50 mHBP	1.04	39.3	75	62

DMTA Analysis

Figure 5 shows the plot of tan δ against temperature determined by DMTA for the binary blends prepared with various content of mHBP. The corresponding parameters[27] such as tan δ, $\triangle T$ for all the formulations are collected in Table II. With the increasing content of mHBP, the T_g shifted to higher temperature and the $\triangle T$ was broaden significantly, especially when 50 phr. mHBP was added, the $\triangle T$ reached 75°C in reference to 54.5°C of the neat crosslinked NBR. When the mHBP content is below 30 phr, the shape of the curve with only one peak indicated a good compatibility between NBR and mHBP; however, when the mHBP content reached 50 phr, a secondary relaxation transition at 75°C is found, corresponding to the enrichment of mHBP, which can be confirmed by SEM [Figure 4(e)]. On the contrary, the NBR/HBP sample exhibited significant heterogeneity, which could be confirmed by two tan δ peaks, even when only 10 phr HBP was added. This phenomenon could be excellently corresponding to the SEM picture [Figure 4(b)]. The TA in T_g was another index for an evaluation of damping performance, indicating that the ability of converting mechanical energy into heat through molecular motion. As shown in Table II, when the mHBP content is 50 phr, the blends obtain the largest TA value, which can keep high tan δ level in a wide temperature range.

Mechanical Properties

The mechanical properties of the crosslinked samples were investigated. The corresponding results, such as tensile strength, elongation at break, permanent deformation, and hardness, were illustrated in Figure 6 and Table III. From the results, it is clear that, when 10 phr HBP was added, the tensile strength decreased significantly from 18.89 MPa to 17.68 MPa caused by the incompatibility between NBR and HBP attributing to the poor interface between the binary phase of NBR and HBP, which can be confirmed by the fracture morphology picture in Figure 4(b).

In contrast, the tensile strength increased from 18.89 MPa to 23.41 MPa with an increase of mHBP content from 0 phr to 30 phr and then decreased slightly with further increasing mHBP content, which can be attributed to the compatibility between NBR and mHBP. The improvement in compatibility may be

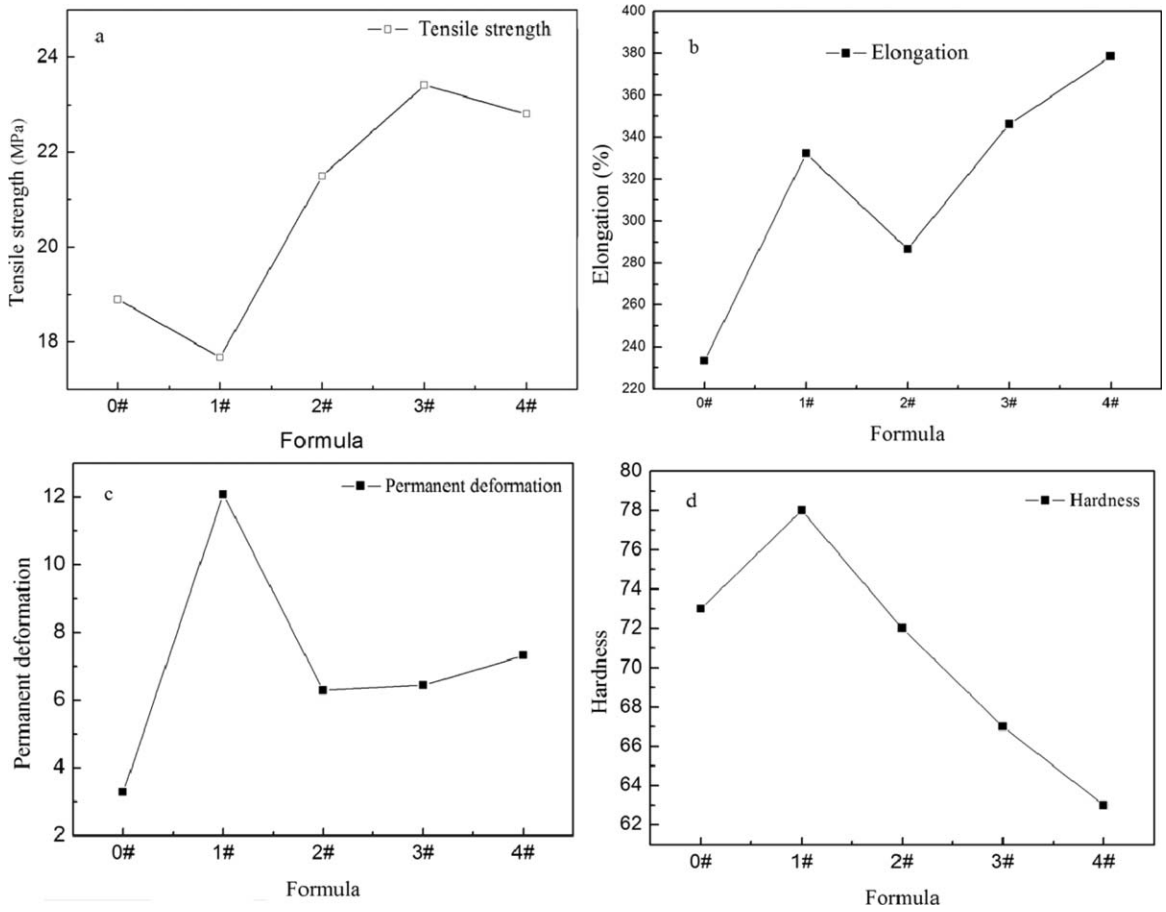

Figure 6. Mechanical properties of NBR/ mHBP blends.

Table III. Mechanical Properties of NBR/mHBP Blends

Materials	Tensile strength (MPa)	Elongation at break (%)	Permanent deformation (%)	Hardness
NBR	18.89	233.4	3.28	73
NBR/10 mHBP	21.50	286.6	6.28	72
NBR/30 mHBP	23.41	346. 1	6.44	67
NBR/50 mHBP	22.81	378.5	7.32	63

attributed to the hydrogen bonds between NBR and mHBP, which can be confirmed in FTIR spectru (Figure 3).

The elongation at break and permanent deformation showed the similar trend of significantly improvement when mHBP (or HBP) was added for all the samples, especially when HBP was added. The main reason for the improvement of elongation at break and permanent deformation may be attributed to the following reasons. First, a hyperbranched polymer, for its short branched molecular chains, exhibits excellent flowing properties, which may increase the motion ability of molecular chains and result in the improvement of elongation at break and permanent deformation. Second, the addition of HBP, as shown in Figure 4(b), led to clearly separation phase, which may decrease the crosslinking density. Third, the hydrogen bonds between NBR and mHBP, confirmed by FTIR spectra (Figure 3), limited the molecular chain motion, which can explain why even more improvement when HBP was added.

The shore hardness improved from 73 to 78 when HBP was added. On the contrary, the hardness decreased from 73 to 62 with the increasing mHBP content from 0 to 50 phr. HBP, dispersed in the NBR in the state of blocks [shown in Figure 4(b)] can be used as rigid filler, which could explain why the hardness improved when HBP was added. While mHBP, showing excellent compatibility with NBR, played an important role in the improvement on molecular chain motion and decrease of crosslinking density, which could explain why the hardness decrease with the increasing mHBP content.

CONCLUSIONS

In this article, hindered phenol exterminated hyperbranched polyester was fabricated through esterification reaction and characterized by FTIR and ^{1}H-NMR. The prepared mHBP was introduced into NBR to prepare NBR/mHBP damping materials. In the temperature dependence of loss factor for the blends, the T_g shifted to higher temperature with the increasing mHBP content, and the $\triangle T$ was broadened from 39°C to 51°C, when the mHBP content reached 50 phr. The FTIR spectra of NBR/mHBP blends proved the existence of intermolecular hydrogen bonding between NBR and mHBP, which played an important role in the damping properties of NBR/mHBP blends. Therefore, the mHBP is expected to have an important application in adjust the T_g and $\triangle T$ of polymer with improved damping properties. The mechanical property results showed that the mHBP played a positive effect on the tensile strength and elongation for the hyperbranched structure of mHBP. Therefore, the mHBP is expected to have an important application of damping and mechanical properties for polymers.

REFERENCES

1. Kaneko, H.; Inoue, K.; Tominaga, Y.; Asai, S.; Sumita, M. *Mater. Lett.* **2002**, *52*, 96.
2. Shi, X.; Bi, W.; Zhao, S. *J. Macromol. Sci. Part B* **2011**, *50*, 1928.
3. Mousa, A.; Heinrich, G.; Simon, F.; Wagenknecht, U.; Stöckelhuber, K.-W.; Dweiri, R. *Mater. Res.* **2012**, *15*, 671.
4. Jaisankar, S. N.; Sankar, R. M.; Meera, K. S.; Mandal, A. B. *Soft Mater.* **2013**, *11*, 55.
5. Shi, X.; Li, Q.; Zheng, A. *Polym. Test.* **2014**, *35*, 87.
6. Xinyan, S.; Weina, B.; Shugao, Z. *J. Macromol. Sci. Part B: Phys.* **2011**, *50*, 1928.
7. Wu, C.; Wei, C.; Guo, W.; Wu, C. *J. Appl. Polym. Sci.* **2008**, *109*, 2065.
8. Perera, S.; Ishiaku, U. S.; Mohd Ishak, Z. A. *Eur. Polym. J.* **2001**, *37*, 167.
9. Zhao, Y.; Zhang, J.; You, S.; He, L.; Zhan, M. *J. Aeronautical Mater.* **2009**, *29*, 71.
10. Xinyan, S.; Weina, B. *J. Macromol. Sci. Part B: Phys.* **2010**, *50*, 417.
11. Liu, Q. X.; Ding, X. B.; Zhang, H. P.; Yan, X. *J. Appl. Polym. Sci.* **2009**, *114*, 2655.
12. Su, C.; He, P.; Yan, R.; Zhao, C.; Zhang, C. *Polym. Compos.* **2012**, *33*, 860.
13. Xiang, P.; Xiao, D.; Zhao, X.; Lu, Y.; Zhang, L. *Acta Materiae Compositae Sinica* **2007**, *24*, 44.
14. Foix, D.; Serra, A.; Amparore, L.; Sangermano, M. *Polymer* **2012**, *53*, 3084.
15. Barua, S.; Dutta, G.; Karak, N. *Chem. Eng. Sci.* **2013**, *95*, 138.
16. Si, J.; Xu, P.; He, W.; Wang, S.; Jing, X. *Compos. Part A: Appl. Sci. Manufacturing* **2012**, *43*, 2249.
17. Bin, S.; Dake, Q.; Guozheng, L.; Aijuan, G.; Li, Y. *Polym. Adv. Technol.* **2013**, *24*, 1051.
18. Ye, J.; Liang, G.; Gu, A.; Zhang, Z.; Han, J.; Yuan, L. *Polym. Degrad. Stab.* **2012**, *98*, 597.
19. Jincheng, W.; Yan, G. *J. Appl. Polym. Sci.* **2011**, *122*, 3474.
20. Yi, Z.; Jincheng, W. *J. Appl. Polym. Sci.* **2013**, *128*, 2385.
21. Dielectric, S. I. *Macromol. Mater. Eng.* **2012**, *297*, 391.
22. Qin, H.; Mather, P. T.; Baek, J. B.; Tan, L.-S. *Polymer* **2006**, *47*, 2813.
23. Bergenudd, H.; Eriksson, P.; DeArmitt, C.; Stenberga, B.; Jonsson, E. M. *Polym. Degrad. Stab.* **2002**, *76*, 503.
24. Wang, X.; Wang, B.; Song, L.; Wen, P.; Tang, G.; Hu, Y. *Polym. Degrad. Stab.* **2013**, *98*, 1945.
25. Jincheng, W.; Yan, G. *J. Appl. Polym. Sci.* **2011**, *122*, 3474.
26. Schüssele, A. C.; Nübling, F.; Thomann, Y.; Carstensen, O.; Bauer, G.; Speck, T.; Mülhaupt, R. *Macromol. Mater. Eng.* **2012**, *297*, 411.
27. Zhao, X.; Xiang, P.; Tian, M.; Fong, H.; Jin, R.; Zhang, L. *Polymer* **2007**, *48*, 6056.